The Mechanism of Reactions Involving Schiff Base Intermediates. Thiazolidine Formation from L-Cysteine and Formaldehyde[1,2]

Roland G. Kallen

Contribution from the Department of Biochemistry, School of Medicine, University of Pennsylvania, Philadelphia, Pennsylvania 19104.
Received August 3, 1970

Abstract: The bell-shaped portion of the pH–rate profile for the reaction of cysteine with formaldehyde to form thiazolidine-4-carboxylic acid (TC) has been shown to result from a change in rate-determining step with changing acidity. In alkaline solution the rate-determining step is the solvent and the solvated proton catalyzed dehydration of an *N*-hydroxymethylcysteine derivative to form a cationic imine intermediate. This step is subject to general acid catalysis with a Brønsted slope, α, of 0.66. In acid solution, attack of cysteine on formaldehyde is rate determining and is not subject to general acid–base catalysis. Thus, the change in rate-determining step can be demonstrated with increasing buffer concentration in the pH region of 6–7. At significant fractions of total cysteine as RSH and relatively high formaldehyde concentration the hemithioacetal forms rapidly and reversibly by either hydronium or hydroxide ion catalyzed pathways prior to the formation of the *N*-hydroxymethyl and cationic imine intermediates in the formation of the thiazolidine. The occurrence of hemithioacetal formation, however, does not make steps beyond Schiff base formation rate determining and the assignment of rate-determining steps for *thiazolidine formation* remains as already noted. Furthermore, TC formation is not inhibited kinetically by a trapping of unhydrated formaldehyde by thiol as unhydrated formaldehyde, the reactive species, is formed from its hydrate. Morpholine catalyzes the reaction of cysteine with formaldehyde to form TC by a pathway which involves nucleophilic catalysis and the intermediate formation of cationic imines, $>^{+}N{=}CH_2$.

Thiazolidine formation from carbonyl compounds and aminothiols has been studied[3] due to its relevance to the binding of carbonyl compounds to proteins containing sulfhydryl and amino groups in close proximity[3d,f,4] (eq 1).

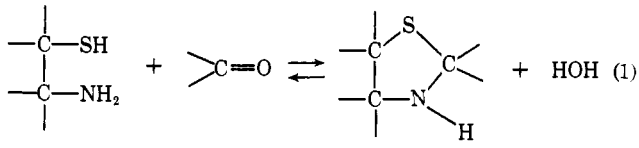

Imidazolidine formation is an analogous reaction which involves an intramolecular aminoalkylation on nitrogen and has been shown to proceed through an addition–elimination sequence to form a cationic Schiff base intermediate II, followed by rapid cyclization to form the final product[5] (Scheme I, path 1, X = N).

Thiazolidine formation has been suggested to proceed through a similar Schiff base intermediate[6] II (path 1, Scheme I, X = S) in the condensation of cysteine with pyridoxal phosphate.[3c,d] The bell-shaped pH–rate profile noted for this system was interpreted in terms of rate-determining cyclization.

An alternative mechanism for thiazolidine formation involves initial attack on formaldehyde by the sulfur atom, the formation of sulfonium ion intermediate, and cyclization (path 3, Scheme I). Two less plausible possibilities involve SN2 displacements of hydroxide from the carbinolamine (path 2) and hemithioacetal[3a,7] (path 4), respectively.

Due to the incomplete nature of the earlier studies, and the lack of kinetic information on reactions of aliphatic amines with aliphatic aldehydes, we have reexamined the mechanism of formation of TC from cysteine and formaldehyde. We have concluded (i) that path 5 is followed when significant fractions of total cysteine exist as RSH and at relatively high formaldehyde concentration (*i.e.*, the hemithioacetal of cysteine forms prior to the *N*-hydroxymethyl and cationic Schiff base intermediates) and (ii) that path 1 is followed under conditions in which hemithioacetal formation is not favorable on thermodynamic grounds. The rate-determining steps for thiazolidine formation in paths 1 and 5 are the formation of the carbinolamine in the acid region and the dehydration of the carbinolamine to form the cationic Schiff base in the alkaline region. A change in rate-determining step occurs in these pathways at about pH 6 from the dehydration

(1) This project was supported by the National Institutes of Health, United States Public Health Service, Grants No. GM 13,777 and FR 15 (University of Pennsylvania Medical School Computer Facility) and FR 05415 (University of Pennsylvania Medical School).

(2) Abbreviations used are: CYS = L-cysteine; CYS_T = total cysteine; $CYS_{RNH_{2T}}$ = cysteine as total amine free base; DABCO = triethylenediamine (1,4-diazabicyclo[2.2.2]octane); EDTA = ethylenediaminetetraacetic acid; F = formaldehyde hydrate, F_F = uncomplexed formaldehyde hydrate, F_T = total formaldehyde hydrate; HEPES = *N*-2-hydroxyethylpiperazine-*N'*-2-ethanesulfonic acid; HFP = hexafluoroisopropyl alcohol; IM = imidazole; IM_T = total imidazole; IMH^+ = imidazolium; M = morpholine free base; $M_H{}^+$ = morpholinium cation; 2-ME = 2-mercaptoethanol; MES = 2-(*N*-morpholino)ethanesulfonic acid; MTHF = N_5,N_{10}-methylenetetrahydrofolic acid; NAC = *N*-acetyl-L-cysteine; N_H = *N*-hydroxymethylmorpholine; $N_{HH}{}^+$ = *N*-hydroxymethylmorpholinium cation; N_D = methylenedimorpholine; $N_{DH}{}^+$ = methylenedimorpholine monocation; SMC = *S*-methyl-L-cysteine; TC = thiazolidine-4-carboxylic acid; THF = tetrahydrofolic acid.

(3) (a) S. Ratner and H. T. Clarke, *J. Amer. Chem. Soc.*, **59**, 200 (1937); (b) D. French and J. T. Edsall, *Advan. Protein Chem.*, **2**, 277 (1945); (c) D. Mackay, *Arch. Biochem. Biophys.*, **99**, 93 (1962); (d) M. V. Buell and R. E. Hansen, *J. Amer. Chem. Soc.*, **82**, 6042 (1960); (e) K. Shinohara, *J. Biol. Chem.*, **110**, 263 (1935); (f) R. G. Kallen, *J. Amer. Chem. Soc.*, **93**, 6227 (1971); and references therein.

(4) J. Heller, *Biochemistry*, **7**, 2914 (1968).

(5) (a) R. G. Kallen and W. P. Jencks, *J. Biol. Chem.*, **241**, 5851 (1966). Discussion of examples of imidazolidine formation in which cyclization may be rate determining will be discussed in a later section;[5b,c] (b) S. J. Benkovic, P. A. Benkovic, and D. R. Comfort, *J. Amer. Chem. Soc.*, **91**, 5270 (1969); (c) S. J. Benkovic, P. A. Benkovic, and R. Chrzanowski, *ibid.*, **92**, 523 (1970).

(6) (a) H. Hellman and G. Opitz, "α-Aminoalkylierung," Verlag Chemie, Weinheim, Germany, 1960; (b) I. E. Pollack, *Chem. Abstr.*, **67**, 116287m (1967); Ph.D. Thesis, Syracuse University, 1967; (c) E. Campaigne, *Chem. Rev.*, **39**, 1 (1946); (d) G. W. Stacy, R. I. Day, and R. J. Morath, *J. Amer. Chem. Soc.*, 77, 3869 (1955).

(7) F. Bergel and K. R. Harrap, *J. Chem. Soc.*, 4051 (1961).

Scheme I

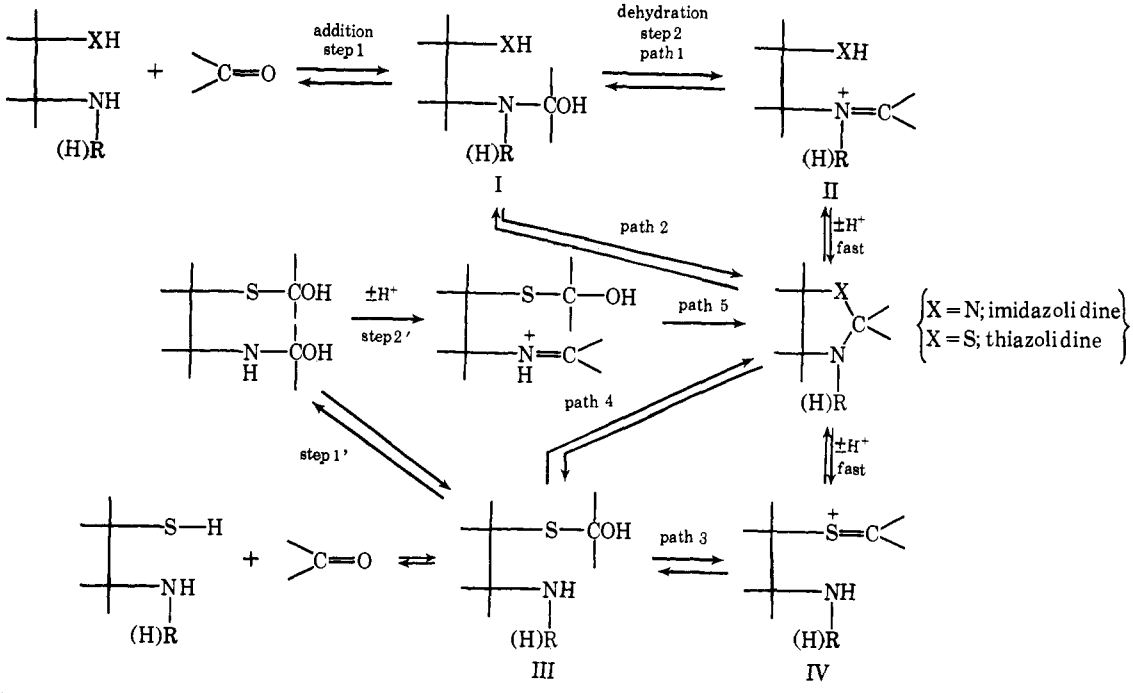

step to the formation of the carbinolamine as the hydronium ion or the buffer concentration is increased and the cyclization step does not appear to become rate determining under any of the experimental conditions examined.

Experimental Section

Materials. Amines were redistilled, converted to the hydrochlorides, and recrystallized or, for DABCO and imidazole, recrystallized as the base from benzene. Other materials have been previously described[3f,5a] and were used without further purification. The final product of the reaction of formaldehyde and cysteine is TC.[3f]

Deionized water (5×10^5 ohms cm specific resistance) was used with potassium chloride to maintain ionic strength. Deuterium oxide was glass distilled prior to use.

Methods. Kinetic Measurements. The rates of reaction of formaldehyde with L-cysteine were followed by measuring the changes in (i) optical rotation[3f] at 546.1 or 589.3 nm or (ii) absorbance at low uv wavelengths. The optimum wavelength for spectrophotometric measurements was determined with split-compartment mixing cells (Pyrocell) by difference spectroscopy between reactants and the formaldehyde adduct. The optical rotatory measurements were made using interference filters in a Bendix automatic polarimeter Model 1100 modified to respond with about a fourfold faster time constant and to utilize a Beckman 10-in. recorder (linear mode, 10 mV scale) with variable scale expansion, zero offset, and a thermostated cell compartment maintained at 25 ± 0.1°.

Absorbance measurements were made in a Beckman DU Model 2000 Gilford or a Hitachi-Coleman Model 124 multiple sample absorbance recorder equipped with cell holders maintained at 25 ± 0.1°. Neutral and alkaline stock solutions of cysteine slowly developed a white precipitate, probably cystine. Therefore, for optical rotatory measurements, stock solutions of 0.1 *M* L-cysteine–HCl were made up daily and added to the reaction mixture (final concentration L-cysteine 0.0025–0.01 *M*) containing buffer, EDTA, and KCl. This reaction mixture (*ca.* 12 ml) was titrated to the pH desired with 1.0 *N* KOH, and immediately added to a 4-cm path-length cyclindrical cell (bubble trap model). After thermal equilibrium was attained, a small volume (<1.2 ml) of formaldehyde solution, at the desired pH, was added and mixed by inversion to initiate the reaction. For spectrophotometric measurements the procedure was similar except that lower concentrations of cysteine and buffer could be used. In the pH range 5–6 the rate of TC formation was also followed titrimetrically (Radiometer Titrigraph SBR2C, AutoBurette ABU 1b, pH meter 26SE with GB2021 electrode standardized with pH 4, 7, and 10 buffers) in thermostated titration vessels by the alkali consumed. Formaldehyde was in sufficient excess to yield pseudo-first-order kinetics and rate constants were obtained from semilogrithmic plots of the difference in measurement at various times, and the final equilibrium measurement against time (*i.e.*, $\Delta M = M_\infty - M_t$ where M_∞ and M_t are the measured rotation, absorbance, or titrant at $t = \infty$ and t = time

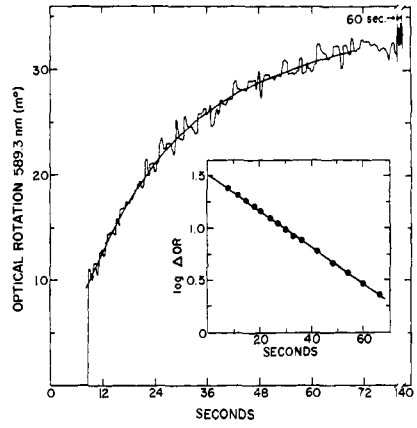

Figure 1. Reaction of L-cysteine (2.5×10^{-3} *M*) with formaldehyde (0.025 *M*), 25°, ionic strength 1.0 *M*, pH 11.26 with 0.2 *M* potassium phosphate buffer, path length 4.0 cm. Inset: logarithmic plot of the same data: $\Delta OR = OR_{final} - OR_t$, where t = time after mixing.

from mixing, respectively) and the equation $k_{obsd} = 0.693/t_{1/2}$ or by the use of digitalized data (Oscar Decimal Converter Model F (Benson-Lehner)) and a computer program to fit log ΔM *vs.* time data by the least-squares method. For high noise level recordings a smooth curve was drawn by hand for analysis (Figure 1). Correlation coefficients were 0.98 for the least precise data and generally better than 0.999; data for at least three half-times were analyzed. The final optical rotation (absorbance) measurements of reaction mixtures and control solutions devoid of formaldehyde showed less than 1% changes over six half-times. The apparent second-order rate constants were obtained from the slopes of plots of k_{obsd} against formaldehyde concentration. The observed total change in rotation (absorbance) for TC formation varied with pH due to differences of specific rotation (molar absorptivity) for the various states of ionization of both cysteine and TC.[3f]

At a given pH, the reaction was shown to proceed to completion by increasing the formaldehyde concentration four- to fivefold;

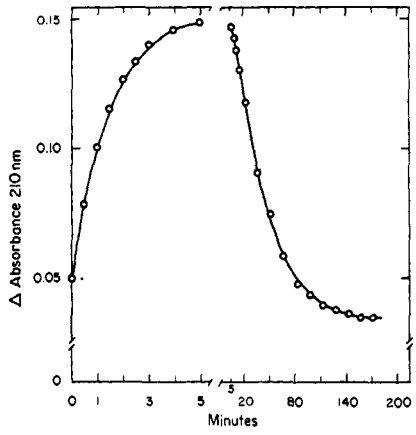

Figure 2. Time dependence of the absorbance change at 210 nm in the reaction of 10^{-3} M L-cysteine with 0.02 M formaldehyde in 0.02 M formate buffer, pH 2.99, ionic strength 1.0 M, 25°.

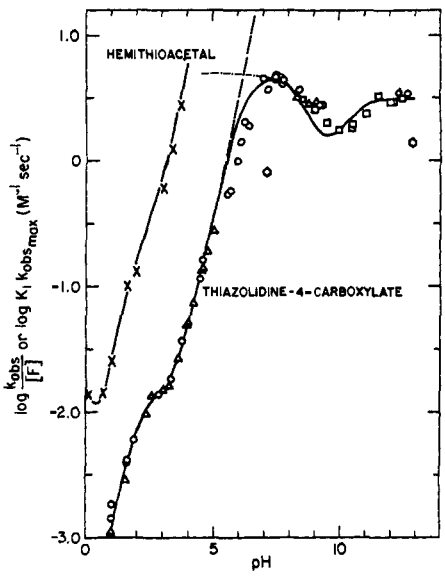

Figure 3. Dependence on pH of second-order rate constants for hemithioacetal (fast-phase absorbance measurements, X) and TC formation (slow-phase absorbance, ○, or optical rotatory, △, measurements). The second-order rate constants were obtained from experiments similar to those illustrated in Figure 4 for linear and in Figure 5 for nonlinear dependence of the pseudo-first-order rate constants on formaldehyde concentration (⊡, optical rotatory; ◈, spectrophotometric). Theoretical curves based on the data in Table II and eq 7,8, and 9 are shown as the dot-dash (-·-), dash (- -), and solid (—) lines, respectively, for TC formation and based on eq 2 for hemithioacetal formation are shown as the solid (—) line. ○, Experiments in deuterium oxide.

the same total change in rotation (absorbance) was observed. Calculations from the equilibrium constants for formation of the respective adducts[3f] confirmed that the reactions proceeded to completion under the experimental conditions employed.

Non-buffer-catalyzed rates were obtained either by extrapolation to zero buffer concentration or by conducting experiments in the presence of buffers which were very poor catalysts. Secondary amine catalysis was studied by the addition of L-cysteine following adjustment of the pH of the reaction mixture of secondary amine and formaldehyde and a 10-min equilibration period to ensure first-order kinetics.[5a] The contribution of the nonnucleophilic-catalyzed free formaldehyde hydrate dependent pathway, $k_0 \times [F_F]/[F_T]$, was subtracted from the observed rates, k_{obsd}, to obtain the amine-catalyzed contribution, where k_0 is the observed rate in the absence of amine and F_F and F_T are free and total formaldehyde hydrate, respectively. Values of $[F_F]$ were calculated from equilibrium constants for formaldehyde adduct formation.[8,9]

Values of pD were obtained from measurements with the glass electrode by adding 0.408 to the observed pH meter readings.[10]

Results

Hemithioacetal Formation from Cysteine. The rate of condensation of cysteine with a large molar excess of formaldehyde, measured spectrophotometrically below 240 nm, is biphasic below pH 4 with an initial rapid first-order increase of absorbance followed by a relatively slow first-order decrease (Figure 2). The difference in rates is such that a spectrum of the solution containing predominantly the intermediate could be obtained (not shown), and the time course of the subsequent spectral changes reveals tight isosbestic points with respect to the spectrum of TC. The formation of hemithioacetal and subsequent transformation of hemithioacetal to TC constitute the first- and second-phase absorbance changes, respectively,[11] Figure 2 (see Discussion). Calculations from equilibrium constants for hemithioacetal formation[12] indicate that this adduct would be expected to form under the experimental conditions employed.

The pseudo-first-order rate constants for the fast first phases of the reaction of cysteine with formaldehyde increase linearly with increasing formaldehyde concentration. This indicates that the rate of this condensation reaction is also first order in respect to formaldehyde concentration.

The pH dependence of the second-order rate constants of the rapid initial reaction of cysteine and formaldehyde for pH 0–4 corresponds to the rate law of eq 2 with respect to total cysteine

$$k_{obsd}/[F] = k_H a_{H^+} + k_{RS_a}\alpha_2 + k_{RS_b}\alpha_{12} \qquad (2)$$

in which α_2 and α_{12} are the fraction of total cysteine as reactive thiol anion species with a carboxylic acid group and a carboxylate group,[13] respectively (Scheme II), and F is formaldehyde hydrate. The solid line drawn through the data for the fast initial reaction of cysteine and formaldehyde (labeled hemithioacetal in Figure 3) is calculated on the basis of eq 2, the α values (Appendix), and the rate constants for hemithioacetal formation from species **2** and **12**, of 7.6×10^4 and 1.8×10^5 M^{-1} sec^{-1}, respectively.[12] The pH dependence of the second-order rate constants of the rapid initial reaction of cysteine and formaldehyde is also quantitatively and qualitatively similar to those for hemithioacetal formation from other thiols, *e.g.*, NAC.[12]

TC is considerably more stable than the hemithioacetal at all pH values studied,[3f] in accord with the above interpretation of the absorbance changes occurring at 210 nm during the formation of TC (Figure 2). The rate of cysteine hemithioacetal formation could not be measured at higher pH values than 4,

(8) R. G. Kallen and W. P. Jencks, *J. Biol. Chem.*, 241, 5864 (1966).
(9) R. G. Kallen, R. O. Viale, and L. K. Smith, *J. Amer. Chem. Soc.*, in press.
(10) P. Salomaa, L. L. Schaleger, and F. A. Long, *ibid.*, 86, 1 (1964).
(11) (a) W. R. Brode, "Chemical Spectroscopy," 2nd ed, Wiley, New York, N. Y., 1943, p 217; (b) L. J. Saidel, A. R. Goldfarb, and S. Waldman, *J. Biol. Chem.*, 197, 285 (1952); (c) E. A. Fehnel and M. Carmack, *J. Amer. Chem. Soc.*, 71, 84 (1949).
(12) R. G. Kallen and M. Frederick, submitted for publication.
(13) The nomenclature for the relevant cysteine species and the microscopic proton dissociation constants is specified in Scheme II (see Appendix for the calculation of the fraction of cysteine as the total amine free base).

Scheme II. Proton Dissociation and Tautomerization Equilibria of Cysteine

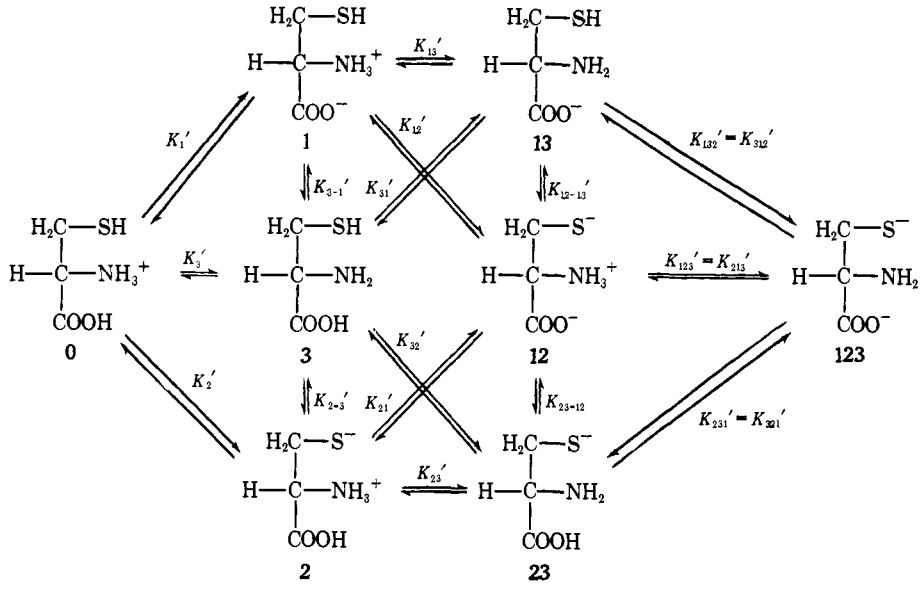

but the inverse relationship with hydrogen ion activity indicates that the rate would be faster than the second kinetic phase, which represents TC formation, in the alkaline region. However, the equilibrium constant for hemithioacetal formation becomes less favorable as the fraction of thiol anion increases.[14] There is indirect evidence for "instantaneous" hemithioacetal formation from pH 4 to 9; the optical rotation extrapolated to zero time does not correspond to the optical rotation of cysteine under conditions in which the discrepancy cannot be accounted for by carbinolamine formation. In addition, in the region of neutrality at extremely low buffer concentrations and 10°, a slight lag in the early part of the reaction occurs which is similar to that observed in MTHF formation in the presence of 2-ME and is the result of a type of kinetic inhibition in which the amine and thiol compete for unhydrated formaldehyde[5a] and hemithioacetal formation is faster than carbinolamine formation.[12]

Thiazolidine Formation from Cysteine. The rate constants for TC formation obtained polarimetrically and, when possible, titrimetrically agree with those obtained from the slower second-phase absorbance changes (Figures 1–3).

No buffer catalysis of TC formation was observed with cyanoacetate (50% free base), formate (9–90% free base), and acetate buffers (9–80% free base), in the concentration range 0.05–0.4 *M* in the pH range 2.3–5.0. However, in the pH region above pH 5.5 catalysis by most buffers contributes significantly to the observed rate and the rate constants in the absence of buffer catalysis were obtained by measuring the rates in duplicate at four or more buffer concentrations at each of a series of pH values and extrapolating to zero buffer concentration at each pH.

The pseudo-first-order rate constants for TC formation were found to increase linearly with increasing formaldehyde concentration in the range 0–0.4 *M* at pH values below 8 (Figure 4, Table I). In the more alkaline region at low formaldehyde concentrations the pseudo-first-order rate constants for the reaction of cysteine with formaldehyde increase linearly with the formaldehyde concentration, but at high formaldehyde concentration at alkaline pH, the rates level off and become independent of the formaldehyde concentration (Figure 5). The leveling off is caused by the complete conversion of cysteine to an intermediate so that a further increase in formaldehyde concentration cannot cause a further increase in the concentration of the intermediate or the rate of its conversion to the final product.[5] The results of a typical experiment are

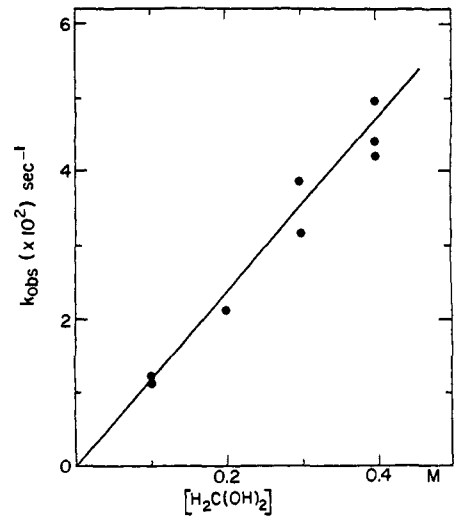

Figure 4. Effect of formaldehyde concentration on the rate of TC formation, 0.01 *M* cysteine at pH 4.60, 0.02 *M* potassium formate, ionic strength 1.0 *M*, 25°.

(14) The pK_a' value for the hemithioacetal of **13** was estimated from a Hammet plot for XCH_2OH compounds ($\rho = -7.29$)[15] and a σ^I value of +0.28 for $HO(CH_2)_2S$– based on the average increment of 0.29 for the difference between alkyl (R–) and alkylthio (RS–) substituent constants and a σ^I value of −0.01 for $CH_3CHOHCH_2$–[16] as a model for $HO(CH_2)_2$–. Based on estimated pK_{a_2} and pK_{a_1} values of 13 and 9.51 for the hemithioacetal and 2-mercaptoethanol itself, respectively, the equilibrium constant for the addition of the thiol anion of 2-ME to formaldehyde ($K = [RSCH_2O^-]/[RS^-][H_2C(OH)_2] = K_H K_{a_2}/K_{a_1}$) is 0.28 M^{-1} where $K_H = [RSCH_2OH]/[RSH][H_2C(OH)_2]$.[12]

(15) (a) R. E. Barnett, "Diffusion Limited Rate-Determining Steps in Carbonyl and Acyl Group Reactions," Ph.D. Thesis, Brandeis University, 1969; (b) P. Ballinger and F. A. Long, *J. Amer. Chem. Soc.*, 82, 795 (1960); (c) R. P. Bell, *Advan. Phys. Org. Chem.*, 4, 15 (1966).

(16) M. Charton, *J. Org. Chem.*, 29, 1222 (1964).

Table I. Dependence of Rate of Thiazolidine-4-carboxylic Acid Formation on Formaldehdye Concentration at 25°, Ionic Strength 1.0 *M*

pH	Buffer: Concn, *M*	Buffer: Free base, %	k_{obsd}[a]/[F], M^{-1} sec^{-1}	$K_{1(app)}$,[b] M^{-1}	$K_{1(app)}/\alpha_{RNH_{2T}}$,[c] M^{-1}	k_2,[d] sec^{-1}	k_{2obsd},[e] sec^{-1}	Formaldehyde concn, *M*
1.00[f,i]	*g*		0.0013					0.1–0.40
1.60[f]	*g*		0.0040					0.1–0.20
2.84[f]	0.01[h]	13	0.014					0.02–0.04
3.35[f]	0.01[h]	37	0.023					0.01–0.02
4.47[f]	0.1[i]	40	0.12					0.0325–0.065
4.59[f]	0.1[i]	47	0.16					0.0325–0.065
4.60[i]	0.02[h]	91	0.12					0.1–0.40
4.77[f]	0.1[i]	57	0.19					0.0325–0.065
5.00[f]	0.1[i]	74	0.27					0.0325–0.065
8.32[i]	0.1[k]	13	3.33					0.025–0.055
8.43[i]	0.1[k]	16		4.4	26.7	*l*	0.67	0.025–0.20
8.97[i]	0.1[k]	39		6.8	25.7	*l*	0.35	0.025–0.20
9.41[i]	0.1[k]	64	1.50					0.025–0.055
9.47[i]	0.1[k]	68		9.6	26.9	*l*	0.21	0.025–0.20
9.95[i]	0.1[k]	86		14.8	31.0	0.12	0.12	0.025–0.20
10.50[i]	0.1[m]	10		15.5	22.2	0.12	0.12	0.025–0.30
10.50[i]	0.1[m]	10		17.8	25.3	0.10	0.10	0.025–0.40
11.08	0.1[m]	30		19.3	21.8	0.12	0.12	0.025–0.40
11.57	0.1[m]	56		20.0	20.9	0.17	0.17	0.025–0.40
					Av 26.8	0.126		
					Stand dev 4.0	0.026		

[a] F = formaldehyde hydrate; linear dependence of rate on formaldehyde concentration. [b] $K_{1(app)}$ is apparent equilibrium constant for carbinolamine formation. [c] $\alpha_{RNH_{2T}}$ is fraction of total cysteine as total amine free base. [d] k_{2obsd} for the pH-independent term in rate law (eq 5) for carbinolamine dehydration is obtained from $k_{obsd_{max}}$ values from saturation curves of rate with respect to formaldehyde concentration at pH >10. [e] $k_{obsd_{max}}$, the apparent pseudo-first-order rate constant for carbinolamine dehydration (Figure 5), includes both solvent and hydronium ion terms. [f] Spectrophotometric method. [g] Hydrochloric acid. [h] Formate. [i] Acetate. [j] Polarimetric method. [k] Triethylenediamine. [l] Hydronium ion catalyzed carbinolamine dehydration is significant below pH 10. [m] Phosphate.

shown in the form of a reciprocal plot (Figure 5) in which the reciprocal of the ordinate intercept is the maximum pseudo-first-order rate constant, $k_{2obsd_{max}}$, at high formaldehyde concentrations (*i.e.*, the rate constant for the conversion of the intermediate to product), the intercept at the abscissa is the negative of the apparent equilibrium constant for the formation of the intermediate, $K_{1(app)}$, and the product of the two constants, $K_{1(app)}k_{2obsd_{max}}$, is the second-order rate constant for the formation of product, *i.e.*, the initial slope of the rectangular hyperbola (Figure 5). The pH dependence of the second-order rate constants for the non-buffer-catalyzed reaction of cysteine and formaldehyde to form thiazolidine obtained from data similar to that in Figures 4 and 5 and Table I under conditions in which the buffer contribution is negligible is shown in Figure 3, with respect to total cysteine concentration, and in Figure 6, with respect to total amine free base.[17,18] There is a sig-

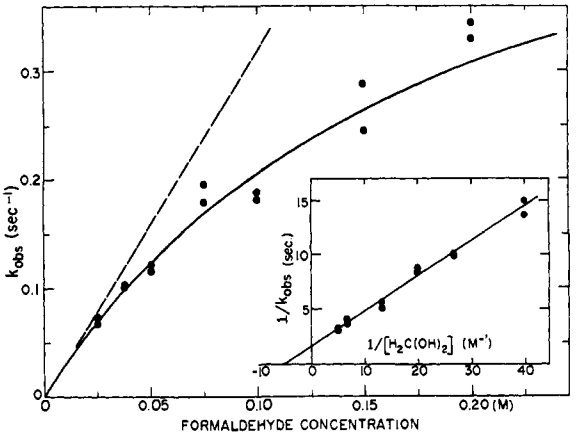

Figure 5. Effect of formaldehyde concentration on the rate of TC formation, 2.5×10^{-3} *M* cysteine at pH 8.43, 25°, ionic strength 1.0 *M*. Reaction conditions: 0.1 *M* triethylenediamine (DABCO), 4.0-cm path length, polarimetric measurements at 546.1 nm. Inset: double reciprocal plot of the pseudo-first-order rate constants against formaldehyde concentration. The calculated lines from the data in Table II and the following equations $k_{obsd} = (k_2 + k_2' \cdot a_{H^+})/(1 + 1/(K_1\alpha_{RNH_{2T}}[F])) = k_{obsd_{max}}/(1 + 1/(K_{1(app)}[F]))$ and $1/k_{obsd} = 1/k_{obsd_{max}} + 1/(k_{obsd_{max}}K_{1(app)}[F])$, respectively, are shown as the *solid lines*.

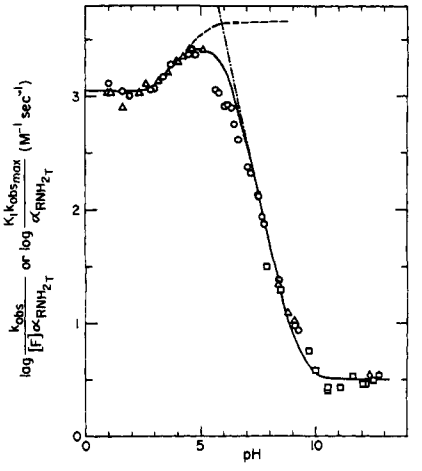

Figure 6. Dependence on pH of the second-order rate constants for thiazolidine-4-carboxylate formation from formaldehyde and L-cysteine as amine free base. Theoretical curves based on constants in Table II and eq 7, 8, and 9 and shown as the dot–dash (–·–), dash (– –), and solid lines (—), respectively.

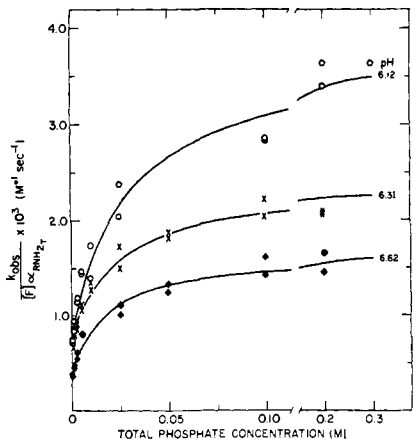

Figure 7. General acid catalysis by phosphate monoanion of the reaction of L-cysteine, as the free base amine, with formaldehyde at pH 6.12 (○), 6.31 (×), 6.62 (◆), ionic strength 1.0 M, and 25°. The *solid lines* are calculated from the coefficients of the least-squares computed fit of the data to the equation, $Y = C_1(C_2 + X/C_3 + X)$ where $Y = k_{obsd}[F]$, $C_1 = k_{1_b}\alpha_{RNH_{2T}}$, $C_2 = k_2'a_{H^+}/(k_2''\alpha_{HA})$, $C_3 = (k_{-1_b} + k_2'a_{H^+})/k_2''\alpha_{HA}$, X is the total buffer concentration, and α_{HA} is the fraction of the total buffer as the acid (eq 10). The coefficients, in order of increasing pH, are: C_1 = 6.24, 6.22, 8.99; C_2 = 6.54 × 10^{-3}, 8.55 × 10^{-3}, 4.24 × 10^{-3}; C_3 = 2.9 × 10^{-2}, 2.62 × 10^{-2}, 1.72 × 10^{-2}. The average values for the rate constants determined from the parameters are: k_1, 2695 M^{-1} sec^{-1}; k_2', 1.87 × 10^8 M^{-1} sec^{-1}; k_2'', 1.22 × 10^4 M^{-1} sec^{-1} (see Tables II and III). The data have been corrected for the fraction of total cysteine as the free base amine, $\alpha_{RNH_{2T}}$. The pH was maintained with 0.03 M MES buffers.

moid-shaped region of the pH–rate profile with respect to the total amine free base in the pH region 0–5 (Figure 6), attributable to the changing state of ionization of the carboxyl group, and different rate constants, k_{1a} and k_{1b}, for species **3** and **13**, respectively (Scheme II).[19] The second-order rate constants, k_{1a} and k_{1b} (Table II), were detemined from the left- and right-

Table II. Apparent Rate and Equilibrium Constants for Reaction of L-Cysteine and Formaldehyde at 25°, Ionic Strength 1.0 M, Water Activity 1.0

$K_1 = \frac{[>NCH_2OH]}{[>NH][F]}$		26.8 ± 4.0 M^{-1} [a]
k_{1a}	$v = k_{1a}[HOOC{\sim}NH_2][F]$	1.11 ± 0.13 × 10^3 M^{-1} sec^{-1}
k_{1b}	$v = k_{1b}[^-OOC{\sim}NH_2][F]$	2.92 ± 0.11 × 10^3 M^{-1} sec^{-1}
k_{-1a}	$v = k_{-1a}[HOOC{\sim}NHCH_2OH]$	4.18 × 10^1 sec^{-1} [b]
k_{-1b}	$v = k_{-1b}[^-OOC{\sim}NHCH_2OH]$	1.05 × 10^2 sec^{-1} [b]
k_2	$v = k_2[>NCH_2OH][HOH]$	0.12 ± 0.012 sec^{-1} [c] 0.126 ± 0.026 sec^{-1} [d]
k_2'	$v = k_2'[>NCH_2OH]a_{H^+}$	1.40 ± 0.05 × 10^8 M^{-1} sec^{-1} [c]

[a] From Table I. [b] Calculated from k_1/K_1. [c] From least-squares fit of second-order constants of Figure 6 and K_1. [d] From $k_{obsd_{max}}$ values obtained as shown in Figure 5 and Table I.

hand intercepts, respectively, of plots of the second-order rate constants for TC formation, with respect to total free-base amine, against the fraction of total free-base amine containing a carboxylate group.

(17) The free base has been shown to be the reactive species in several related systems.[18]

(18) (a) W. P. Jencks, "Catalysis in Chemistry and Enzymology," McGraw-Hill, New York, N. Y., 1969; (b) W. P. Jencks, *Progr. Phys. Org. Chem.*, 2, 63 (1964).

(19) Species **23** and **123** of cysteine (Scheme II) constitute a negligible fraction of the total in this pH region and the assignment of a significant portion of the observed rate to **123** is inconsistent with the pH–rate profile in Figures 3 and 6.

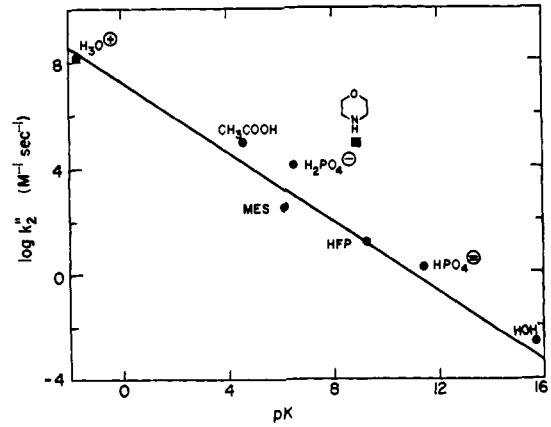

Figure 8. Brønsted plot for general acid catalysis of dehydration of an *N*-hydroxymethyl intermediate I of L-cysteine at 25°, ionic strength 1.0 M, where rate = $k_2''[>NCH_2OH][HA]$. The line is a least-squares fit of the points for general acid catalysts and has a slope α = 0.66 ± 0.07. The point for morpholine, obtained at low concentrations, is calculated as if it were a general acid catalyst; this compound functions by a nucleophilic catalytic pathway and was not included in calculations of the slope.

Catalysis of the reaction of cysteine with formaldehyde by buffers at pH values greater than 8 is proportional to the acid species of the buffer with the rate constants corrected to the species of cysteine as the amine free base (not shown) in accord with the rate law

$$v_{cat} = k_{HA}\alpha_{RNH_{2T}}[CYS_T][F][HA] \quad (3)$$

in which v_{cat} is the rate of the buffer-catalyzed reaction, $\alpha_{RNH_{2T}}$ is the fraction of cysteine as the total amine free base (see Appendix), and CYS_T is total cysteine. However, this rate law is kinetically indistinguishable from the rate law

$$v_{cat} = \frac{k_{HA}\alpha_{RNH_3^+}}{K_{HA}'}[CYS_T][F][A^-] = k_{cat}'[RNH_3^+][F][A^-] \quad (4)$$

in which K_{HA}' is the ionization constant for the acid catalyst and $\alpha_{RNH_3^+}$ is the fraction of cysteine as the protonated amine. Since cysteine is largely in the ammonium ion form under conditions in which catalysis by buffers is observed, the observed rates of the catalyzed reaction in terms of the total cysteine increase with increasing pH, according to this rate law (eq 4).

The catalytic constants for a number of acids are summarized in Table III. The values for the solvated proton and for water were calculated from the data shown in Figure 6 and the rate law

$$\text{rate} = K_1k_2[CYS_{RNH_{2T}}][F][HOH] + K_1k_2'[CYS_{RNH_{2T}}][F]a_{H^+} \quad (5)$$

which describes the rate of the reaction, exclusive of buffer catalysis, in the alkaline region with respect to total amine-free base cysteine, $CYS_{RNH_{2T}}$, and is shown by the dot-dashed line at the right in Figure 6.

For catalysis by phosphate buffers, there are two–threefold increases in rate from 0 to 0.025 M buffer, but as the buffer concentration is further increased, the apparent catalytic constant diminishes to zero and the line levels off at a constant pH (Figure 7). This leveling off is another reflection of the mechanism

Table III. Second-Order Rate Constants for General Acid Catalysis of Dehydration of *N*-Hydroxymethylcysteine at 25° [a]

Catalyst	pH	Concn range, *M*	No. of expt	Fraction HA	pK_a'	k_2'', M^{-1} sec^{-1} [b]
H_3O^+	7.5–9.5		34		−1.7	1.4×10^8
Acetic acid	5.72	0.001–0.20	15	0.07	4.60	9.3×10^4 [d]
2-[*N*-Morpholino]ethanesulfonate (MES)	6.44–7.02	0.01–0.30	18	0.20–0.39	6.13	2.5×10^2
Phosphate monoanion	6.12–6.62	0.001–0.3[c]	47	0.43–0.68	6.50	1.2×10^4 [d]
Hexafluoro-2-propanol (HFP)	9.26–9.74	0.05–0.40	22	0.35–0.50	9.22	1.4
Phosphate dianion	10.47	0.05–0.30	12	0.90	11.42[e]	0.17
HOH	9.5–13		8		15.7	0.12/55.5

[a] Ionic strength maintained at 1.0 *M* with potassium chloride. [b] From $k_2'' = (k_{obsd} - k_{nbc})/\alpha_{RNH_2T}[F][HA]K_1$, where k_{nbc} is the non-buffer-catalyzed rate, F is formaldehyde hydrate, K_1 is the equilibrium constant for *N*-hydroxymethylcysteine formation from cysteine and formaldehyde, $[CYS_T]$ is the total cysteine, and $v_{HA}/K_1\alpha_{RNH_2T} = k_2''[CYS_T][F][HA]$. [c] pH maintained with 0.03 *M* MES. [d] From least-squares fit of curves as in Figure 7. [e] pK_a' is concentration dependent at constant ionic strength.

Table IV. Pseudo-First-Order Rate Constants for Morpholine-Catalyzed Thiazolidine-4-carboxylate Formation from Total Amine Free-Base Cysteine as Function of Morpholine Concentration[a]

pH	Total morpholine, *M*	Free[b] formaldehyde × 10^2 *M*	$\frac{k_{obsd} - \frac{k_0[F_F]}{[F_T]}}{\alpha_{RNH_2T}}$, sec^{-1}	k^*/a_{H^+}[c] × 10^9, M^{-2} sec^{-1}
6.38[d]	0.075	1.87	5.3	3.58
	0.10	1.69	6.81, 7.95	3.63, 4.24
	0.20	1.10	13.8, 15.3	4.56, 5.05
	0.30	0.66	18.0	5.02
				Av 4.3 ± 0.7
7.22[e]	0.025	1.85	1.52, 1.86	4.4, 5.4
	0.05	1.38	3.08, 3.31	5.6, 5.3
	0.075	1.06	4.10, 4.23	5.4, 5.7
	0.10	0.83	4.16, 4.38	5.0, 5.3
	0.20	0.33	4.94	5.2
	0.30	0.13	5.52	6.7
				Av 5.4 ± 0.6
8.35[f]	0.002	2.33	0.002, 0.032	3.0, 4.3
	0.003	2.25	0.0412, 0.066	3.9, 6.0
	0.005	2.09	0.121, 0.121	6.8, 6.8
	0.010	1.72	0.22, 0.26	7.5, 6.5
	0.015	1.38	0.36	7.4
	0.02	1.09	0.41	6.7
				Av 5.9 ± 1.6
9.25[g]	0.002	2.31	0.008, 0.013	7.2, 12.0
	0.003	2.21	0.025, 0.025	15.6, 15.6
	0.005	2.03	0.054, 0.063	23.7, 20.4
	0.01	1.57	0.104, 0.095	19.9, 18.2
	0.03	0.31	0.133, 0.138	14.3, 13.8
				Av 16.1 ± 5

[a] Total formaldehyde hydrate 0.025 *M*, 10°, ionic strength 1.0 *M*. [b] The equilibria of morpholine and formaldehyde involve the species M, M_{H^+}, N_H, N_{HH^+}, N_D, and N_{DH^+}; for abbreviations see ref 2, and for the calculations of the composition of such solutions see ref 9. [c] $k^* = \{k_{obsd} - k_0[F_F]/[F_T]\}/\{\alpha_{RNH_2T}[N_H]\}$. [d] α_{RNH_2T}, k_0 (sec^{-1}) (applies to footnotes *e*–*g* also); 0.00132, 0.020. [e] 0.00883, 0.025. [f] 0.0853, 0.026. [g] 0.228, 0.023.

which causes the bell-shaped pH–rate profile in the pH region 5–9.5 (Figure 3).

Morpholine is far more effective at low concentrations than are other catalysts of similar pK_a' value for the reaction of cysteine with formaldehyde (Figure 8). However, as the concentration of secondary amine is increased, there is a leveling off and, at some pH values, an inhibition of the rate at high amine concentrations. The rate of the secondary amine-catalyzed reaction of cysteine, as the amine free base, to form the thiazolidine was found to be directly proportional to the hydroxymethylmorpholine and hydrogen ion activity in the pH range 6.38–9.25 (Table IV), although at the highest pH the values of k^*/a_{H^+} appear to be slightly higher for unknown reasons.

Imidazole fails to function as a nucleophilic catalyst for the formation of thiazolidine (*cf.* ref 5a) and, due to its ability to bind formaldehyde,[8] causes inhibition of the rate of TC formation (Table V). The major fraction of the observed rates can be accounted for in terms of the formaldehyde not bound to imidazole as indicated by the second-order rate constants calculated with respect to the concentration of free formaldehyde hydrate (Table V). The small trend upward in the corrected rate constants with increasing imidazole concentration is consistent with a small general acid catalytic contribution by imidazolium with $k_2'' \sim 6 \times 10^3$ M^{-1} sec^{-1} (*cf.* Table III).

Table V. Pseudo-First-Order Rate Constants for Thiazolidine-4-carboxylate Formation from Cysteine as a Function of Imidazole Concentration[a]

	Total imidazole, *M*						
	0.00	0.05	0.10	0.15	0.20	0.25	0.30
$k_{obsd} \times 10^2$ sec^{-1}	2.0	1.30	0.90	0.75	0.62	0.54	0.52
		1.23	0.89	0.74	0.63	0.58	0.48
$k_{obsd}/[F_F]$ M^{-1} sec^{-1} [b]	0.60	0.63	0.66	0.64	0.64	0.66	0.73
		0.60	0.65	0.63	0.65	0.71	0.67

[a] pH 7.79; 25°; ionic strength 1.0 *M*; imidazole, 75% free base; L-cysteine, 3×10^{-4} *M*; total formaldehyde hydrate, 3.3×10^{-3} *M*. [b] F_F = free formaldehyde hydrate; F_T = total formaldehyde hydrate; IM_T = total imidazole; calculated from the following equation obtained from detailed balance in formaldehyde: $2K_2'[IM_T](1.0 - \alpha_{fb})[F_F]^2 + \{1 + K_1[IM_T]\alpha_{fb} + K_2[IM_T](1.0 - \alpha_{fb})\}[F_F] - [F_T] = 0$ where $K_1 = [>NCH_2OH]/[IM][F_F]$, $K_2 = [HIM^+CH_2OH]/[IMH^+][F_F]$, $K_2' = [IM^+(CH_2OH)_2]/[IMH^+][F_F]^2$, and α_{fb} is the fraction of imidazole as the free base. The values of the equilibrium constants K_1, K_2, and K_2' are 15 M^{-1}, 3.2 M^{-1}, and 2.3 M^{-2}, respectively (ref 8).

Discussion

Formaldehyde Dehydration. For carbonyl compounds, the reactive form toward nucleophilic attack is the unhydrated species.[5a,12,15c,20–22] The linearity

(20) (a) G. E. Lienhard and W. P. Jencks, *J. Amer. Chem. Soc.*, **88**, 3982 (1966); (b) R. E. Barnett and W. P. Jencks, *ibid.*, **89**, 5963 (1967); (c) R. E. Barnett and W. P. Jencks, *ibid.*, **91**, 6758 (1969).

(21) E. G. Sander and W. P. Jencks, *ibid.*, **90**, 6154 (1968).

(22) (a) R. P. Bell and P. G. Evans, *Proc. Roy. Soc. (London), Ser. A*, **291**, 297 (1966); (b) P. LeHénaff, *C. R. Acad. Sci. Paris*, **256**, 1752 (1963); (c) P. Valenta, *Collect. Czech. Chem. Commun.*, **25**, 853 (1960).

of the data in first-order plots for thiazolidine formation with total formaldehyde in large molar excess provides evidence that formaldehyde hydrate dehydration is not rate determining (Figure 1).

Reliable confirmation that formaldehyde hydrate dehydration has not been partially or completely rate determining was obtained by simulations of the reaction with the kinetic parameters for formaldehyde hydrate dehydration[22a,b] and TC formation and demonstration that the free unhydrated formaldehyde concentration is insignificantly perturbed during product formation for the range of experimental conditions reported in this study. Furthermore, the pH–rate profile (Figure 3) is inconsistent with a rate-determining step involving formaldehyde hydrate dehydration which is hydronium ion catalyzed below pH 4 and hydroxide ion catalyzed above pH 7.[22a,b]

Hemithioacetal Formation from Cysteine and Formaldehyde. The mechanism of the reaction of thiols with carbonyl compounds to form hemithioacetals has been well characterized,[12,18,20] and the characteristics of the reaction of formaldehyde with cysteine (first phase, Figure 2), which occurs more rapidly than TC formation, are in accord with the assignment of the first phase to hemithioacetal formation: (1) first-order dependences of the rate of hemithioacetal formation on the aldehyde concentration;[12,20] (2) hydrogen and hydroxide ion catalyzed limbs of the pH–rate profile[12,20] for hemithioacetal formation, perturbed in the cases of NAC[12] and cysteine by the changing ionization state of the carboxyl group in the pH regions of 3.2 and 2.4, respectively; (3) rate constants for thiol anion attack on formaldehyde for 2-ME and for both carboxylic acid and carboxylate species of NAC and cysteine which fall very close to the line correlating rate with basicity for aliphatic thiols varying more than 10^4 in basicity, β value 0.18;[12] (4) (a) slight lags in the rate of TC formation which occur at very low buffer concentrations and lower temperature at about pH 7 and are consistent with competition between thiol and amine for unhydrated formaldehyde as it formed;[5a] (b) the observation that above pH 5.5 the absorbance changes with 2-ME, NAC, and cysteine (fast phase) conform to zero-order kinetics which indicates that formaldehyde hydrate dehydration has become rate determining;[12,20a] (5) similarities in the spectral shifts for methylation and hydroxymethylation, *i.e.*, comparison of spectra of thiols[11a,b] with alkyl sulfides,[11b] alkoxy sulfides,[11c] and hemithioacetals,[12] below 240 nm; (6) the magnitude and pH dependence for the equilibrium constants for *N*-hydroxymethylamine, cationic Schiff base, hemithioacetal, and thiazolidine formation.[3f,20b,c] Finally, there is correspondence of the rates of the second-phase spectrophotometric changes with optical rotatory and titrimetric measurements of TC formation. Alternative formulations for the biphasic absorbance changes for cysteine (Figure 2) which have been considered cannot account for the observations noted above.

Significance of the pH–Rate Profile for Reaction of Cysteine and Formaldehyde. The leveling off in the rate of thiazolidine formation (Figure 3) at about pH 7 with an apparent pK_a' of about 6 in the bell-shaped pH–rate profile (pH region 5–9) does *not* correspond to any of the proton dissociation constants of cysteine (Scheme II, Appendix).[3f] The bell-shaped pH–rate profile in this region must be, therefore, partly an expression of the kinetics of the reaction rather than simply of the ionization constants of the reactants. These data resemble the bell-shaped pH–rate profiles observed in an increasing number of carbonyl group reactions[5,18,23,24] including thiazolidine formation from cysteine and pyridoxal derivatives,[3d,7] and is the result of a change in rate-determining step with pH. The pH–rate profile in the region of pH 5–9 may be most simply described as rate-determining attack of the nucleophilic reagent on the carbonyl group in one pH region and rate-determining dehydration of the resulting addition product, the carbinolamine I, to form the Schiff base II in another pH region (paths 1 or 5, Scheme I) as shown in eq 6. Further evidence favoring these paths over other paths of Scheme I will be presented in a later section.

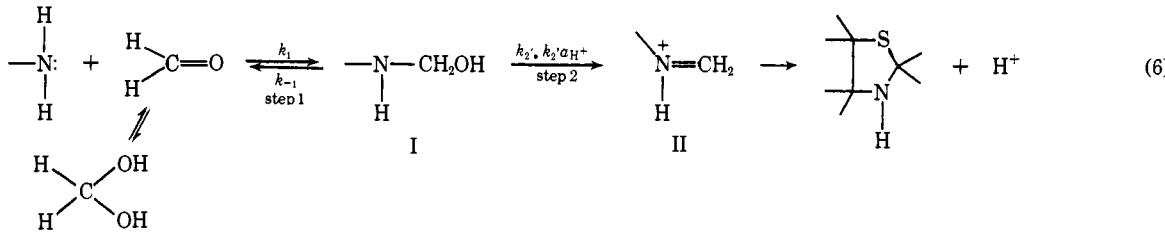

(6)

It is probable that the intramolecular attack of the sulfur atom on the cationic imine in the last step of the reaction is fast (see below), as is the cyclization reaction in MTHF formation.[5a] That it is the cationic rather than neutral imine which is subject to intramolecular nucleophilic attack in the cyclization step is supported by considerable data on analogous reactions which involve nucleophilic attack on Schiff bases.[26]

The dependence of the rate on pH provides evidence for a change in rate-determining step, but does not show which step is rate determining in each pH region. Analogy with condensations of other reactions of carbonyl groups with nitrogen compounds suggests that dehydration of the carbinolamine is rate determining at alkaline pH.[18] The dehydration step is acid catalyzed, which accounts for the increasing rate with decreasing pH in the pH region 9–7 (Figure 6), but as this rate becomes very fast with increasing acidity, the rate of amine attack which is not acid catalyzed

(23) W. P. Jencks, *J. Amer. Chem. Soc.*, **81**, 475 (1959).

(24) G. E. Lienhard and W. P. Jencks, *ibid.*, 87, 3855 (1965), and references therein.

(25) It has been suggested that there is a change in rate-determining step with pH in alkaline phosphatase catalyzed reactions.[25a,b] (a) H. N. Fernley and P. G. Walker, *Nature (London)*, **212**, 1435 (1966); (b) W. N. Aldridge, T. E. Barman, and H. Gutfreund, *Biochem. J.*, **92**, 23C (1964).

(26) (a) K. Koehler, W. Sandstrom, and E. H. Cordes, *J. Amer. Chem. Soc.*, **86**, 2413 (1964); (b) E. H. Cordes and W. P. Jencks, *ibid.*, 84, 832 (1962); (c) E. H. Cordes and W. P. Jencks, *ibid.*, **84**, 826 (1962); (d) E. H. Cordes and W. P. Jencks, *ibid.*, **85**, 2843 (1963).

can no longer keep up with carbinolamine dehydration and amine attack becomes rate determining. Above pH 9, the dehydration step is solvent catalyzed, as observed in other related systems,[26a,b,c,27,28a,b] and the pH–rate profile (Figure 3) reflects the changing ionization state of cysteine. The rate of the attack step increases with increasing pH in the region below pH 7 (Figure 3) in which the amine is protonated, because the free-base form of the amine is the reactive species, while the rate of the dehydration step is independent of pH because the decreased rate of the solvated proton-catalyzed dehydration of the carbinolamine is balanced by the increased equilibrium concentration of the addition intermediate with decreased acidity caused by an increased concentration of cysteine as the free base.

Evidence that this assignment of rate-determining steps is correct for the reaction of cysteine with formaldehyde at alkaline pH values is the leveling off of the rate with increasing formaldehyde concentration at pH 8 and above (Figure 5). Thus, when cysteine is completely converted to the *N*-hydroxymethyl adduct, a further increase in the formaldehyde concentration cannot result in a further rate increase and the rate of dehydration of the intermediate may be observed directly.[28c] The equilibrium constant for the formation of this adduct, obtained from a series of reciprocal plots of data similar to that shown in Figure 5, is 26.8 M^{-1}, when corrected to the free base amine (Table II), and corresponds to the range of values of 15.9–25.9 M^{-1} for a carbinolamine formation from formaldehyde and a series of similar primary amino acids including *S*-methyl-L-cysteine.[3f,8] The fact that saturation kinetics were observed to pH values of 13.3, with similar values of K_1, a pH at which there is insignificant interaction between thiolate anions and formaldehyde at the concentrations employed,[14] supports the interpretation that carbinolamine formation is the basis for the independence of rate on formaldehyde concentration (Figure 5) at these and lower pH values.[29]

At the acid and alkaline extremes of the pH–rate profile, one or the other of the two steps is completely rate determining and the observed rate may be accounted for by the relatively simple rate laws for these individual steps (eq 7 and 8).

At alkaline pH, where acid- and solvent-catalyzed dehydration is rate determining, the rate law is

$$\text{rate} = k_2[\text{I}][\text{HOH}] + k_2'[\text{I}]a_{\text{H}^+} \quad (7a)$$

$$= (K_1k_2[\text{HOH}] + K_1k_2'a_{\text{H}^+})[\text{CYS}_\text{T}][\text{F}]\alpha_{\text{RNH}_2\text{T}} \quad (7b)$$

in which I is an *N*-hydroxylmethylcysteine derivative. The calculated line for this rate law based on the measured equilibrium constant for adduct formation and the rate constants for its dehydration (Table II) is shown as the dot–dashed lines on the right sides of Figures 3 and 6 for the observed data and that corrected to the total free base amine, respectively, based on eq 7b.

The fact that this rate law is not followed in the pH region below 6 means that there is a pH-independent addition of the free-base amine forms of cysteine to formaldehyde, so that the rate law in this region is

$$\text{rate} = \{k_{1a}\alpha_a + k_{1b}(1.0 - \alpha_a)\}[\text{CYS}_\text{T}][\text{F}]\alpha_{\text{RNH}_2\text{T}} \quad (8a)$$

$$\text{rate} = \{k_{1a}\alpha_3 + k_{1b}\alpha_{13}\}[\text{CYS}_\text{T}][\text{F}] \quad (8b)$$

where $\alpha_a = \alpha_3/(\alpha_3 + \alpha_{13})$, *i.e.*, fraction of total amine free base cysteine with an un-ionized carboxyl group. This is consistent with previous observations that for basic amines the net neutral zwitterionic carbinolamine, $>\text{N}^+\text{HCH}_2\text{O}^-$, breaks down to amine and carbonyl compound; complete proton removal to form the alkoxide is necessary to expel the leaving group.[18] The dashed lines on the left sides of Figures 3 and 6 are based on eq 8b and the rate constants in Table II, and agree satisfactorily with the observed rates in the pH region below 5.5.

At intermediate regions of pH, both steps are partially rate determining and the rate can be described only by the use of a rate equation (eq 9) based on the

$$k_{\text{obsd}} = \frac{(k_{1a}\alpha_3 + k_{1b}\alpha_{13})[\text{F}]}{\left\{\dfrac{k_{1a}\alpha_3/K_1 + k_{1b}\alpha_{13}/K_1}{k_2 + k_2'a_{\text{H}^+}}\right\} + 1} \quad (9)$$

mechanism of eq 6 and the application of the steady-state approximation to the carbinolamine intermediate. The calculated rate based on this equation and the rate constants in Table II is shown as the solid line in Figures 3 and 6, and shows satisfactory agreement with the observed rate constants.

Further evidence for a change in rate-determining step comes from the dependence of the rate on buffer concentration at a constant pH. At pH 6.12, 6.31, and 6.62, the reaction is catalyzed by phosphate buffers at low phosphate concentration, but shows a tendency to level off at higher buffer concentrations (Figure 7). The step which is subject to catalysis by general acids at higher pH is the carbinolamine dehydration step and this is the step which shows catalysis at low buffer concentrations just below pH 7; however, as the buffer concentration is increased in this pH region, the dehydration step becomes faster and the attack step, which is not subject to buffer catalysis, becomes largely rate determining, as has been observed in related reactions.[5a,18,30]

The steady-state rate eq 10 may be derived from the scheme of eq 6, by including the rate constant for buffer catalysis, $k_2''[\text{HA}]$, for the dehydration step. The solid

$$k_{\text{obsd}} = \frac{(k_{1a}\alpha_3 + k_{1b}\alpha_{13})[\text{F}]}{\left\{\dfrac{k_{1a}\alpha_3/K_1 + k_{1b}\alpha_{13}/K_1}{k_2 + k_2'a_{\text{H}^+} + k_2''[\text{HA}]}\right\} + 1} \quad (10)$$

lines of Figure 7 were calculated from nonlinear least-squares fits of the data and average values for the rate constants calculated from these coefficients are in satisfactory agreement with the rate constants obtained from

(27) (a) T. C. French and T. C. Bruice, *Biochemistry*, **3**, 1589 (1964); (b) A. Williams and M. L. Bender, *J. Amer. Chem. Soc.*, **88**, 2508 (1966); (c) M. Masui and C. Yijima, *J. Chem. Soc. B*, 56 (1966).

(28) (a) E. H. Cordes and W. P. Jencks, *Biochemistry*, **1**, 773 (1962); (b) W. P. Jencks and E. H. Cordes, *Chem. Biol. Aspects Pyridoxal Catal. Proc. Symp. Int. Union Biochem.*, **1962**, 57 (1963); (c) it was not experimentally feasible to form the adduct at alkaline pH and show a faster rate of thiazolidine formation upon rapidly plunging the reaction mixture into an acidic medium by conventional methods.

(29) There is no significant *N*-dihydroxymethylcysteine formed both on the basis of the equilibrium constant for its formation from the monohydroxymethyl adduct for SMC (ref 3 f) and the fact that the kinetic data were satisfactorily fit as rectangular hyperbolae with respect to formaldehyde concentration.

(30) E. H. Cordes and W. P. Jencks, *J. Amer. Chem. Soc.*, **84**, 4319 (1962).

analysis by least-squares methods of the experimental data in this and other pH regions (Table II).

General Acid Catalysis of the Dehydration Step. The rate of the dehydration step of the *N*-hydroxymethyl adduct was too fast at saturating formaldehyde concentration for the precise measurement of second-order catalytic constants. Third-order rate constants, K_1k_2'', for the general acid catalyzed dehydration step, with respect to total amine free base were measured under conditions first order in respect to formaldehyde concentration, and second-order catalytic constants for the rates of dehydration in terms of the carbinolamine intermediate were calculated based on $K_1 = 26.8\ M^{-1}$.

Although the dehydration step is subject to general acid catalysis,[31] limited data could be collected for the following reasons: (a) the attack step becomes totally rate determining below pH 5, (b) there are relatively stringent steric and charge requirements for general acid catalysts, and (c) the Brønsted coefficient, α, is 0.66, with or without statistical corrections (Figure 8), consistent with the experimental fact that catalysis by the weaker acids is of comparatively little importance; catalysis by the solvated proton or solvent is dominant. The difference between this α value and the value of close to, if not, zero for data in the pH region below 5 is further evidence for the difference in the nature of the rate-determining steps at alkaline and acid pH.

The probable mechanisms[35] of the general acid catalyzed dehydration step or its microscopic reverse, the attack of water on an imine, are shown in transition states V and VI.

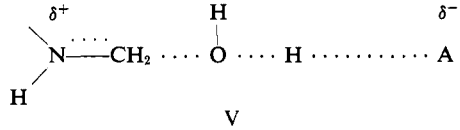

V

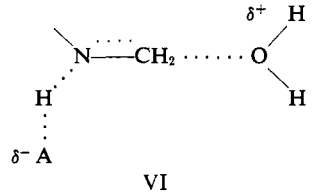

VI

Transition state V depicts general acid catalysis, aiding the hydroxide leaving as water, while transition state VI depicts the kinetically indistinguishable mechanism which involves protonation of the leaving hydroxyl group in a prior equilibrium and general base catalysis by removal of the proton from the nitrogen atom concomitantly with the expulsion of water. The mechanism of transition state V is preferred based on the similarity in the Brønsted $\alpha = 0.66$ (Figure 8) to the range of α values, 0.73–0.77, for a series of secondary amines in which the second mechanism is not possible.[5a,26,36] The large α values indicate that the extent of proton transfer in the transition state is probably large, *i.e.*, the proton is near the oxygen. One would expect that in order for the energy maximum to occur late in proton transfer the acceptor atom would be considerably less basic than the proton-donating acid; this would occur in the case in which proton transfer is at equilibrium in the transition state only if the amount of C–O bond cleavage were small in the transition state of the dehydration step.[26d] More detailed discussions of the location of the proton in the transition state of general acid catalyzed reactions have recently appeared.[20a,b,36,37]

The rate of dehydration of the carbinolamines in the present study appears to be insensitive to the state of the neighboring thiol and a single pair of rate constants, k_2 and k_2' (eq 5), appears to be adequate for the three neighboring groups RSH, $RSCH_2OH$, and RS^-. TC formation proceeds predominantly through dehydration of *S*,*N*-dihydroxylmethyl-L-cysteine to form the Schiff base in the pH range in which hemithioacetal formation is thermodynamically favorable, which contradicts previous assignments of hemithioacetal species as "dead-end" complexes.[3c] The calculated second-order rate constant for the solvated proton-catalyzed dehydration of *N*-hydroxymethyl-L-cysteine must be $1.0 \times 10^{11}\ M^{-1}\ sec^{-1}$ to account for the observed rate of product appearance if the productive pathway proceeds only through *N*-hydroxymethylcysteine, and this value is larger than the diffusion-controlled limit for reactions other than that of the solvated proton with hydroxide ion, species of opposite charge and abnormally high mobility.[38] Beyond the rate-determining steps for Schiff base formation, either (i) base-catalyzed hemithioacetal breakdown (which occurs at rates which are close to diffusion controlled[12,20]) and cyclization to form TC are fast steps or (ii) attack of the hemithioacetal sulfur atom on the cationic Schiff base is a fast step in TC formation.

Carbinolamine Formation. The logarithms for the second-order rate constants for free-base amine attack on unhydrated formaldehyde for diethylamine,[39] trimethylamine,[40] phenylephrine,[41] and cysteine (species **13** and **3**) are 7.46, 7.11, 7.31, 6.83, and 6.41, respectively. The slope for the correlation of basicity with nucleophilicity for these amines, expressed according to the Brønsted equation,[18a] is 0.21. This indicates that for this range of moderately to strongly basic amines (pK_a' range 6.88–10.98) there is relative insensitivity of nucleophilicity to basicity, which may reflect partly the counterbalance between greater nucleophilicity and greater steric inhibition with increasing alkyl substitution[36] and partly a rather small amount of N–C bond formation in the transition state.

(31) Correction of the data obtained in deuterium oxide in Figure 3 based on $\Delta pK = pK_{H_2O} - pK_{D_2O}$ values of −0.60 for $>^+ND$,[32] −0.24 for $-SD$,[15a,20a] and 0.52 for $-COOD$[33] for the microscopic proton dissociation constants of cysteine (see Appendix) yields a $K_1k_2'(H_2O)/K_1k_2'(D_2O)$ value of 1.4 and a $K_1k_2(H_2O)/K_1k_2(D_2O)$ value of 2.2. If it is assumed that there is little deuterium isotope effect on K_1[34] the kinetic deuterium isotope effects are 1.38 and 2.29 for $k_{2_{H_2O}}'/k_{2_{D_2O}}'$ and $k_{2_{H_2O}}/k_{2_{D_2O}}$, respectively. Both experimental and theoretical uncertainties regarding the magnitude of isotope effect and the occurrence of inverse isotope effects[34] in reactions which involve proton transfers of this kind make the interpretation of these data inconclusive at present.

(32) W. M. Schubert and Y. Motoyama, *J. Amer. Chem. Soc.*, **87**, 5507 (1965).

(33) C. A. Bunton and V. J. Shiner, Jr., *ibid.*, **83**, 42 (1961).

(34) B. M. Anderson and W. P. Jencks, *ibid.*, **82**, 1773 (1960).

(35) Mechanisms in which proton transfer alone is the rate-determining step are unlikely for similar reactions.[18a,30]

(36) J. E. Reimann and W. P. Jencks, *J. Amer. Chem. Soc.* **88**, 3973 (1966).

(37) L. do Amaral, W. A. Sandstrom, and E. H. Cordes, *ibid.*, **88**, 2224 (1966).

(38) M. Eigen, *Angew. Chem., Int. Ed. Engl.*, **3**, 1 (1964).

(39) J. DeLuis, "The Chemistry of Formaldehyde–Amine Condensation Products," Ph.D. Thesis, Pennsylvania State University, 1964; *Chem. Abstr.*, **63**, 8184d (1964).

(40) J. Hine and F. C. Kokesh, *J. Amer. Chem. Soc.*, **92**, 4383 (1970).

(41) R. G. Kallen, unpublished experiments.

Scheme III

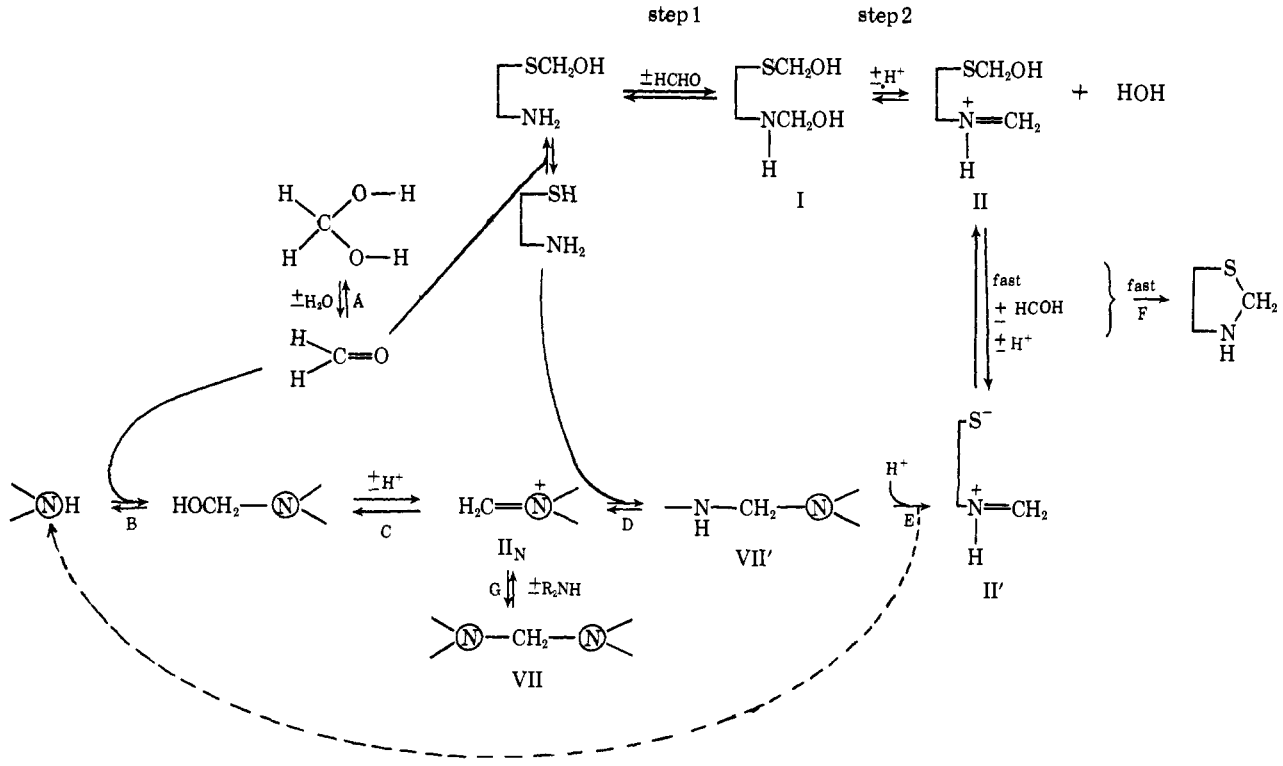

The mechanism for the attack step[18b] is represented in eq 11.

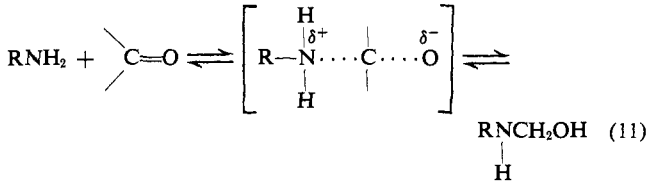

(11)

Since k_{1a} is less than k_{1b} (Table II) and neither rate constant shows unusual deviations from the Brønsted plot (not shown) for carbinolamine formation from a series of amines and formaldehyde, intramolecular neighboring group participation by the adjacent carboxylic acid or the carboxylate groups in the attack step is undetectable.

Catalysis by Morpholine. The catalytic constant for morpholine catalysis of thiazolidine formation from cysteine and formaldehyde indicates that this secondary amine is more than three orders of magnitude more effective than other general acid–base catalysts of similar pK_a' values (Figure 8) and probably functions by a different mechanism. Nucleophilic catalysis of the reactions of amines with carbonyl compounds has been observed in several related reactions.[5a,18a,28] The fact that the rate of the amine-catalyzed reaction increases with increasing acidity when expressed with respect to cysteine as the free base (Table IV) indicates that the secondary amine catalyst and formaldehyde react to form a hydroxymethylamine >Ⓝ-CH_2OH, which undergoes dehydration to give the reactive cationic imine intermediate, >Ⓝ$^+$=CH_2 (Scheme III). This intermediate reacts with the amine nitrogen atom of cysteine to give the same cationic imine, II, as in the uncatalyzed pathway, which rapidly undergoes ring closure to give TC. The rate of the TC formation is inhibited at high concentrations of amine (catalyst) by the formation of the unreactive methylenediamine, VII, from formaldehyde and two molecules of secondary amine.[5a,8] The second-order rate constants for the morpholine-catalyzed reaction with respect to cysteine as the free base and total hydroxymethylmorpholine concentration[9] are contained in Table IV. Within experimental error, the rate of the catalyzed reaction follows the concentration of hydroxymethylmorpholine linearly at a given pH; linearity is not observed if the rates are analyzed with respect to methylenedimorpholine concentration.

The above evidence permits the conclusion that the transition state for the catalyzed reaction contains the elements of hydroxymethylmorpholine, cysteine, and a proton under conditions in which the morpholine–formaldehyde equilibria have been attained by prior equilibration. The rate-determining step in Scheme III, therefore, can be either D, the reaction of the cationic imine with cysteine, or E, the acid-catalyzed expulsion of morpholine from the intermediate, VII. Studies of transaldimination reactions[26a] suggest that attack is the rate-determining step for the reaction of weakly basic amines with Schiff bases derived from strongly basic amines. The similarity in basicity of morpholine[9] (pK_a' 8.88) and cysteine (pK_{13}' 8.90) and the complex dependence of rates on polar substituents and basicity[18a] make it difficult, at present, to deduce which is the rate-determining step in the morpholine-catalyzed thiazolidine formation pathway. A similar difficulty has arisen in the case of the methoxyaminolysis of benzylideneanilines.[37]

The rapid rate of the catalyzed reaction shows that the ring closure in the final step of the reaction is not rate determining in the uncatalyzed reaction because the catalyzed reaction proceeds at a much faster rate and involves the same intermediate. Similar considerations have been applied to the formation of N_5,N_{10}-methylene-THF by uncatalyzed and nucleophilic-

catalyzed pathways[5a] in which the cyclization step is also fast. Nucleophilic catalysis provides one type of kinetic evidence for the existence of cationic imines in aqueous solution.[42] Another type of kinetic evidence has been provided by studies of imidazolidine formation from formaldehyde and tetrahydroquinoxaline derivatives in water–dioxane (50:50) based on the interpretation that ring closure has become the rate-determining step with certain compounds in acid.[5b,c] More direct evidence for the general features of paths 1 and 5 (Scheme I), including the existence of cationic imines in aqueous solution and fast ring closure, has been obtained from studies of the hydrolysis of oxazolidines,[43a] *S*-ethyl-α-dimethylaminobenzyl sulfide,[32] and thiazolidines[43b] in acid solution in which ring opening with Schiff base formation is rapid to form a spectrophotometrically observable benzylideneaniline. It is the subsequent hydrolysis of the Schiff base which is largely or completely the rate-determining step in these systems at pH values greater than 1.

That ring closure is not the rate-determining step in the alkaline region contradicts earlier conclusions for the reaction of cysteine derivatives with pyridoxal phosphate[3d] and a reinvestigation of this reaction will be reported separately.

The evidence that substitution reactions on carbon atoms bonded to oxygen or nitrogen and to one or two more oxygen, nitrogen, or sulfur atoms proceed in highly polar solvents, such as water, by elimination–addition mechanisms,[18] analogous in these cases to A1 pathways, has led to our rejection of paths 2 and 4 (Scheme I). The pH–rate profile is also not easily reconciled with paths 2 and 4, Scheme I.

Although sulfur has the ability to provide some stabilization of an adjacent carbonium ion[44] through resonance contributions by trivalent sulfonium canonical forms, $-S^+{=}C<$, which permit the possibility of path 3 (Scheme I), as suggested by Ratner and Clarke[3a] and Bergel and Harrap,[7] there is evidence which makes this pathway unlikely. The marked unreactivity of mercaptals of substituted thiols,[45–47] which require extreme conditions for formation and, once formed, are quite kinetically stable under conditions in which linear methylenediamines[8,9] and imidazolidines[5] form and hydrolyze with facility, can be attributed largely to the greater stability and/or ease of formation of cationic imine, $>C{=}N^+<$, than of the sulfonium ion, $-S^+{=}C<$, intermediates. The remarkable difference in reactivity of mercaptals and methylenediamines cannot be attributed to marked differences in the leaving abilities of alkylthiol anions and alkylamines since the leaving abilities of these groups are probably not sufficiently different.[48]

Although the hemithioacetal of cysteine is formed rapidly enough to be an intermediate, it is apparent from the present data that the formation of the carbinolamine, while somewhat slower than hemithioacetal formation and thermodynamically less favorable in the pH range investigated by Ratner and Clarke,[3a] is also sufficiently rapid to enable it to be a kinetically competent intermediate and that path 3 is not mandatory (*cf.* ref 3a).[49] Thus this reaction may proceed through a pathway with kinetically significant but not readily detectable concentrations of an intermediate and failure to observe the carbinolamine in acid solution by optical rotation measurements does not rule out a pathway which involves that intermediate.

Since formaldehyde reacts rapidly with aminothiols to form thiazolidines, the suggestion that the formol titration technique[51] be utilized to aid the assignment of pK_a' values to amino and thiol groups in the same molecule appears to be of dubious value.

Acknowledgments. We gratefully acknowledge the contributions of Drs. Judith Oslick and Paul Cohen, and, especially, Mrs. Linda Smith Greenwald and Joan Braun to this work. Special appreciation is due to Drs. Richard O. Viale and Gustav E. Lienhard for their interest and helpful discussion.

Appendix

The general expression for the fraction of the total that exists as any species, C_x, or sum of species, ΣC_x, is $\Sigma\alpha_x = \Sigma[C_x]/\text{total}$, where x is one of the subscripts in Scheme II, and can be calculated for the cysteine species as a function of pH by the following relations: $F_1 = K_1'/a_{H^+}$, $F_2 = K_2'/a_{H^+}$, $F_3 = K_3'/a_{H^+}$, $F_{13} = (K_{13}'/a_{H^+})F_1$, $F_{12} = (K_{12}'/a_{H^+})F_1$, $F_{23} = (K_{32}'/a_{H^+})F_3$, $F_{123} = (K_{123}'/a_{H^+})F_{12}$, $\alpha_0 = 1.0/(1.0 + F_1 + F_2 + F_3 + F_{13} + F_{12} + F_{23} + F_{123})$. Then $\Sigma\alpha_x = \Sigma F_x\alpha_0$, and $\alpha_{RNH_{2T}} = \alpha_3 + \alpha_{23} + \alpha_{13} + \alpha_{123} = (F_3 + F_{23} + F_{13} + F_{123})\alpha_0$; where the relevant microscopic proton dissociation constants at 25 and 10°, respectively, are: pK_1' = 2.00, 2.03; pK_2' = 7.44, 7.71; pK_3' = 6.88, 7.24; pK_{12}' = 8.54, 8.81; pK_{13}' = 8.90, 9.26; pK_{32}' = 8.88, 9.15; pK_{123}' = 10.22, 10.58 (ref 3f). The enthalpies

(42) (a) E. C. Wagner, *J. Org. Chem.*, **19**, 1862 (1954); (b) F. M. Huennekens, H. R. Whiteley, and M. J. Osborne, *J. Cell. Comp. Physiol.*, **54** (suppl. 1), 109 (1959).

(43) (a) T. H. Fife and L. Hagopian, *J. Amer. Chem. Soc.*, **90**, 1007 (1968); (b) T. H. Fife and L. H. Brod, *ibid.*, **91**, 4217 (1969); see footnote 23, p 4219.

(44) (a) D. S. Tarbell and D. P. Harnish, *Chem. Rev.*, **49**, 1 (1951); (b) N. Kharasch, Ed., "Organic Sulfur Compounds," Vol. 1, Pergamon Press, New York, N. Y., 1961; (c) C. C. Price and S. Oae, "Sulfur Bonding," Ronald Press, New York, N. Y., 1962; (d) W. A. Pryor, "Mechanisms of Sulfur Reactions," McGraw-Hill, New York, N. Y., 1962.

(45) The assumptions that mercaptal formation occurs readily in aqueous solution on the basis of indirect spectrophotometric data[3c,7] are probably invalid.

(46) (a) E. Baumann, *Ber.*, **18**, 883 (1885); (b) T. Posner, *ibid.*, **36**, 296 (1903).

(47) E. Campaigne and J. R. Leal, *J. Amer. Chem. Soc.*, **76**, 1272 (1954).

(48) The rate constants for the predominant aqueous pathways of the breakdown of the respective formaldehyde adducts, namely, hydroxide ion catalyzed decomposition of the neutral hemithioacetal of 2-mercaptoethanol and the uncatalyzed decomposition of net neutral formocholine (pK_a' = 9.3), are $3.3 \times 10^6\ M^{-1}\ sec^{-1}$ and $3.4 \times 10^3\ sec^{-1}$, respectively. Since almost complete proton removal from the hemithioacetal (pK_a' estimated to be 13, ref 14) by hydroxide ion is necessary to expel the leaving thiol anion, the first-order rate constant for decomposition is $3.3 \times 10^5\ sec^{-1}$. These calculations suggest that the thiol anion has a leaving ability of roughly a hundredfold greater than trimethylamine.

(49) (a) For monothioacetal hydrolysis, which proceeds through an A1 mechanism, if hydronium ion catalyzed C–O cleavage was tenfold slower than C–S cleavage (in order to account for the fact that no C–O cleavage is observed), the calculated rate constant for hydronium ion catalyzed formation of the sulfonium ion intermediate is less than $2.5 \times 10^{-3}\ M^{-1}\ sec^{-1}$.[49b] Based on this rate constant, the calculated rate of TC formation by a hydronium catalyzed pathway is 10^{10} slower than the observed rate and is evidence against path 3, Scheme I. The mechanisms of paths 1 and 5 (Scheme I) are also supported by the similarity of the present data with that for Schiff base formation from methylamine and isobutyraldehyde.[50] (b) T. H. Fife and E. Anderson, *J. Amer. Chem. Soc.*, **92**, 5464 (1970).

(50) (a) J. Hine, F. A. Via, J. K. Gotkis, and J. C. Craig, Jr., *ibid.*, **92**, 5186 (1970); (b) J. Hine, J. C. Craig, Jr., J. G. Underwood, II, and F. A. Via, *ibid.*, **92**, 5194 (1970).

(51) S. Lewin, *Biochem. J.*, **64**, 30P (1956).

of ionization used to calculate the pK' values at 10° were the following: +0.76 kcal/mol (alanine) for carboxylic acids,[52] +9.13 kcal/mol (SMC) for ammonium groups,[3f] and +6.9 kcal/mol (2-mercaptoacetic acid) for thiol groups.[53,54]

(52) J. T. Edsall and J. Wyman, "Biophysical Chemistry," Vol. I, Academic Press, New York, N. Y., 1958.

(53) (a) R. E. Benesch and R. Benesch, *J. Amer. Chem. Soc.*, 77, 5877 (1955); (b) R. Cecil and J. R. McPhee, *Biochem. J.*, **60**, 496 (1955).

(54) D. P. Wrathall, R. M. Izatt, and J. J. Christensen, *J. Amer. Chem. Soc.*, **86**, 4779 (1964).

New Synthesis and Absolute Configuration of Tetrahydroisoquinoline Cactus Alkaloids

Arnold Brossi, John F. Blount, Jay O'Brien, and Sidney Teitel*

Contribution from the Chemical Research Department, Hoffmann-La Roche Inc., Nutley, New Jersey 07110. *Received March 4, 1971*

Abstract: The 7,8-methylenedioxy-substituted alkaloids, (−)-anhalonine (**3**) and (−)-lophophorine (**4**), have been prepared by a new and facile synthesis which utilized the 7,8-diphenol **6** as the key intermediate. X-Ray crystallographic studies of **3**·HBr and **11**·HBr established that both **3** and **4** as well as the related alkaloid (+)-*O*-methylanhalonidine (**11**) possess the *S* configuration.

In connection with the structure elucidation of the four major tetrahydroisoquinolines found in the peyote cactus, Späth and coworkers synthesized (±)-anhalonidine[1] (**1**), (±)-pellotine[1] (**2**), (−)-anhalonine[2,3] (**3**), and (−)-lophophorine[2,3] (**4**). Since this classic study, alternate methods have been developed for the preparation of the 6,7-dimethoxy-8-hydroxy-substituted alkaloids **1** and **2**[4] but not for the 6-methoxy-7,8-methylenedioxy-substituted alkaloids **3** and **4**. We now describe a novel and simplified synthesis of **3** and **4** which is based on the partial O-demethylation of the 6,7,8-trimethoxy-substituted tetrahydroisoquinoline **5** to provide the corresponding (±)-6-methoxy-7,8-diphenol **6** as the key intermediate.[5]

Treatment of (±)-*O*-methylanhalonidine[6] (**5**) with 20% hydrochloric acid under controlled conditions afforded the 6-methoxy-7,8-diphenol **6**[5] which was reacted with ethyl chloroformate to yield the carbamate **7**. Cupric oxide catalyzed condensation of **7** with dibromomethane in dimethylformamide[7] provided the methylenedioxy derivative **8** which was either converted into (±)-anhalonine (**9**) by base-catalyzed hydrolysis or into (±)-lophophorine (**10**) by lithium aluminum hydride reduction. Alternatively, **10** was also obtained by the reductive condensation of **9** with formaldehyde in the presence of Raney nickel catalyst. Resolution of **9** with (−)-tartaric acid according to the procedure of Späth and Kesztler[3] afforded the alkaloid (−)-anhalonine (**3**) which was transformed by N-methylation into natural lophophorine (**4**).

Although both **3** and **4** have been assigned the *S* configuration by the method of optical rotatory shifts,[8] this approach appeared unreliable for the related tetrahydroisoquinoline (+)-*O*-methylanhalonidine (**11**). The latter alkaloid, a minor constituent in the peyote cactus, was prepared from **5** by resolution with (+)-tartaric acid[9] and exhibited an anomalous optical behavior in solvents of different polarity. Unlike **3** and **4**, **11** showed the same molecular rotation in both chloroform and 1 *N* hydrochloric acid. In view of this, it was deemed advisable to confirm the absolute configurations of **3** and **4** and establish that of **11** by X-ray crystallography. For this purpose, **3**·HBr and **11**·HBr were chosen for study.

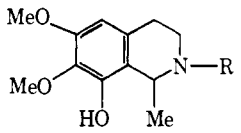

1, R = H
2, R = Me

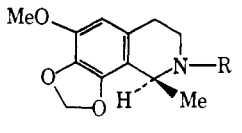

3, R = H
4, R = Me

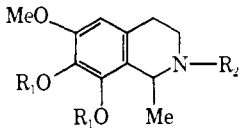

5, R_1 = Me; R_2 = H
6, R_1 = R_2 = H
7, R_1 = H; R_2 = CO_2Et

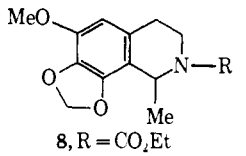

8, R = CO_2Et
9, R = H
10, R = Me

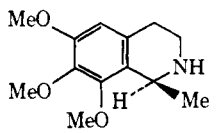

11

Pertinent results of the crystallographic studies are shown in Figures 1, 2, and 3. Bond lengths and angles involving the nonhydrogen atoms of **3**·HBr[10] and **11**·

(1) E. Späth, *Monatsh. Chem.*, 43, 477 (1922); E. Späth and F. Becke, *Chem. Ber.*, 67, 266 (1934).
(2) E. Späth and J. Gange, *Monatsh. Chem.*, 44, 103 (1923).
(3) E. Späth and F. Kesztler, *Chem. Ber.*, 68, 1663 (1935).
(4) A. Brossi, F. Schenker, and W. Leimgruber, *Helv. Chim. Acta*, 47, 2089 (1964); M. Takido, K. L. Khanna, and A. G. Paul, *J. Pharm. Sci.*, 59, 271 (1970).
(5) A. Brossi and S. Teitel, *Chem. Commun.*, 1296 (1970).
(6) S. Karady, *J. Org. Chem.*, 27, 3720 (1962).
(7) M. Tomita and Y. Aoyagi, *Chem. Pharm. Bull.*, **16**, 523 (1968).
(8) A. R. Battersby and T. P. Edwards, *J. Chem. Soc.*, 1214 (1960).
(9) E. Späth and J. Bruck, *Chem. Ber.*, 72, 334 (1939).
(10) The bond lengths have been averaged over the thermal motion with one atom assumed to ride on the other; see W. R. Busing and H. A. Levy, *Acta Crystallogr.*, 17, 142 (1964).